Electronic Supplementary Information for *Energy & Environmental Science*

Enhanced thermal conductivity of phase change materials with ultrathin-graphite foams for thermal energy storage

Hengxing Ji,† Daniel P. Sellan,† Michael T. Pettes, Xianghua Kong, Junyi Ji, Li Shi* & Rodney S. Ruoff*

†***These authors contributed equally to this work***

Department of Mechanical Engineering and Materials Science and Engineering Program, The University of Texas at Austin,
1 University Station C2200, Austin, Texas 78712, United States.

Received (in XXX, XXX) Xth XXXXXXXXX 20XX, Accepted Xth XXXXXXXXX 20XX
DOI: 10.1039/b000000x

Ultrathin-graphite foam (UGF) and composite synthesis. The UGF was fabricated by saturating the nickel foam template with carbon and subsequent precipitation of graphite on its surface during cool-down. The nickel foam (INCOFOAM^{TM}, Novamet Specialty Products Corp., 42 mg cm^{-2} foam density, 450 µm average pore size, and 1.7 mm thickness) was cut into ~4 cm by ~10 cm strips and loaded into a 1 inch fused quartz tube in a hot wall furnace (TF55035A-1, Linderburg/Blue M). The nickel foam was positioned at the center of the furnace. The quartz tube was evacuated, then filled with a gas mixture of Ar (50 sccm, 99.999%, Airgas) and H_2 (10 sccm, 99.999%, Airgas) until the chamber reached atmospheric pressure. The furnace was ramped to a temperature of T = 1050 °C at atmospheric pressure under flowing Ar (50 sccm) and H_2 (10 sccm). The nickel foam was annealed under H_2 for 30 minutes before introducing CH_4 (99.999 %, Airgas). Exposure for 60 minutes at T = 1050 °C to 40 sccm Ar, 5 sccm CH_4 and 5 sccm H_2 was followed by cool-down at a rate of 10 °C min^{-1} to room temperature. The graphite-coated nickel foam was subsequently placed in 0.5 M $(NH_4)_2S_2O_4$ (Aldrich) aqueous solution at T = 80 °C for 10 days and then gently washed in several baths of deionized water, and finally rinsed in isopropanol before drying at T = 50 °C in ambient condition. The UGF samples were weighed (XP105DR, Mettler Toledo), and the sizes of the UGF were measured with a vernier caliper. The volume fraction of UGF samples were calculated by dividing the density of the UGF by that of HOPG (2.26 g/cm^3).

The UGF-composite samples were prepared by drop casting UGF into a vat of hot liquid PCM. Paraffin wax (Aldrich) and food-grade erythritol (local grocery store) were melted on a hotplate (Thermal Scientific) at a temperature of 100 and 140 °C, respectively. The UGF was placed in liquid wax without any treatment, but the UGF was treated by a plasma treatment (Plasma Preen II, Kurt J. Lesker) for 40 seconds in oxygen at a pressure of

1 torr before immersing into hot liquid erythritol. The filled UGF was then taken out of the liquid PCM after about 5 seconds and cooled to room temperature in room air.

Structural characterization. The scanning electron microscopy was carried out on a Quanta 600 FEG (acceleration voltage of 30 kV for UGF and of 2 kV for UGF-composite, FEI Company). The diffraction interference contrast imaging was carried out on an Axio Scope (Carl Zeiss). The micro-CT scanning was carried out on microXCT-200 (50 kV X-ray energy, 23 seconds acquisition time per frame, 931 scanning frames with 1 μm resolution, Xradia, Inc.). Raman spectroscopy was carried out on an Alpha 300 (100×, 0.9 NA, objective lens and 488 nm laser excitation, WITEC GmbH). Thermal Gravity Analysis was performed using a TGA4000 (temperature ramping rate of 5 °C/min, Perkin Elmer).

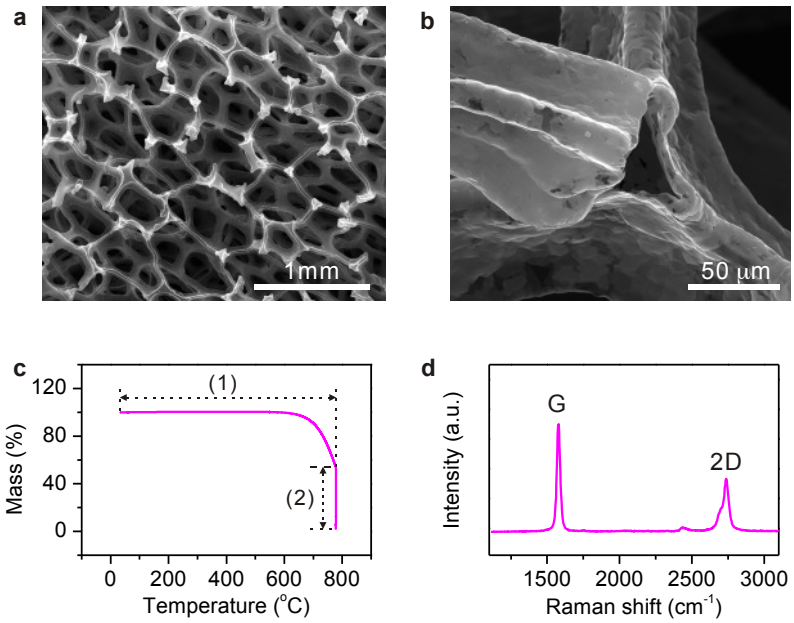

Figure S1. (a, b) Scanning electron micrographs showing ultrathin-graphite foam (UGF) made of 3D interconnected graphite struts. (c) Thermal gravimetric analysis of UGF, which was carried out by heating the UGF sample in air at a ramping rate of 5 °C min^{-1} (curve 1) followed by holding the temperature at 780 °C for 30 minutes (curve 2), shows a final mass residual of 1.2 wt.%, indicating a successful removal of nickel. (d) A typical Raman spectrum of UGF.

Electrical measurement. We used a four-probe technique to measure the electrical resistance of the UGF-composite samples. Figure 2a in the manuscript shows a photograph of the UGF-composite placed on a hotplate (ECHOTHERM™ HS60) with programmable temperature control. A Keithley 2611A current source is used to supply a current sweep, and a Keithley 6514 voltmeter is used to probe the voltage drop. The resistance is obtained from the V-I curve. To ensure good electrical contact with the UGF, the electrodes were attached to the UGF using silver epoxy (see Fig. 2a in the manuscript) before filling with PCM.

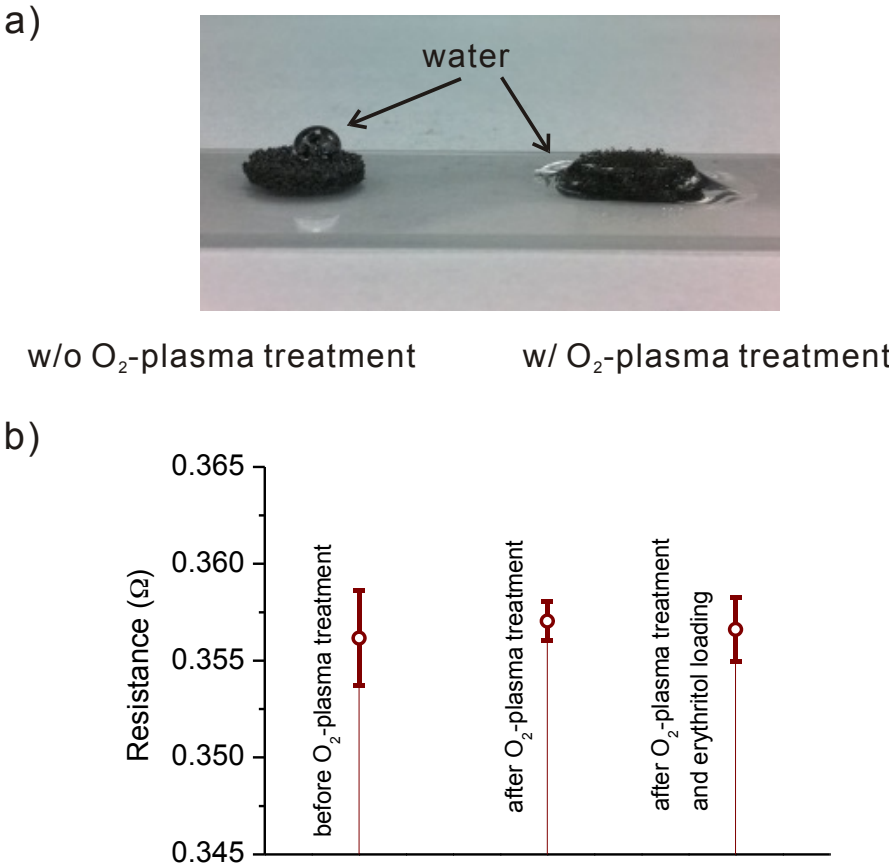

Figure S2. (a) Photograph of two ultrathin-graphite foams: before (left) and after (right) O_2-plasma treatment. The water droplet stayed on the UGF that was not treated with O_2-plasma, while the foam sample with O_2-plasma treatment was wetted by water immediately. (b) The electrical resistance measured at 135 °C by the four-probe method of an UGF sample before O_2-plasma treatment, after O_2-plasma treatment, and after erythritol loading, all for the same sample. The electrical resistance change of the UGF foam after the O_2-plasma treatment and after erythritol loading is within the random error of three independent measurements with different sweep current ranges.

Figure S3. Photograph of bulk erythritol to illustrate the large crystallite size.

UGF-composite stability test. The UGF-composite was heated to a temperature of 100 °C for molten wax loading, and was treated with O_2-plasma then heated to 135 °C for molten erythritol loading. The sample temperature was cycled between 30 and 100 °C for UGF-wax and 75 to 135 °C for UGF-erythritol at a heating and cooling rate of 5 °C min^{-1}. The sample resistance was recorded by using the four-probe configuration described above when the PCMs were at their liquid and solid states for every 5 cycles (see Figs. 2d and 2e in the manuscript).

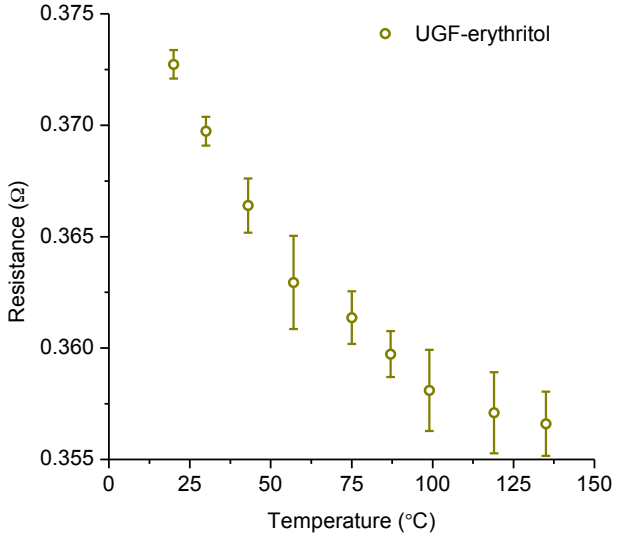

Figure S4. Electrical resistance of UGF-erythritol composite measured at different temperatures.

Heat of fusion measurements. The heat of fusion for the pure PCMs and their composites was measured using differential scanning calorimetry (Netzsch DSC-404 F1 Pegasus). Figure 3 presents DSC measurement data for the melting of food-grade erythritol and UGF-erythritol composite for a heating ramp rate of 10 °C/min. The melting temperature of erythritol and UGF-erythritol composite are nearly identical at T_m = 120.2 ^{o}C. The heat of fusion data presented in manuscript Figs. 3b and 3c and supplementary Table S1 are calculated as the average of Melt 2 and Melt 3. The heat of fusion of the UGF-erythritol composite is 98.6±3.5% of the erythritol value of ΔH_{fus} = 338.5±10.2 J g^{-1}, and within the experimental error of the measurement.

Thermal conductivity measurements

Self-electrical-heating measurements. We used a self-electrical-heating steady state technique to measure the thermal conductivity of our suspended unfilled UGFs and their composites. Details of the measurement technique are found in Ref. 24 and a photograph of a mounted sample is shown in Supplementary Fig. S5. For each measurement, a four-probe electrical resistance versus temperature curve is first measured. The sample is then Joule-heated using direct current, and the average temperature rise is found using the measured electrical resistance and the generated electrical resistance versus temperature curve. The applied Joule-heat generation and corresponding average temperature rise are then used with a one-dimensional heat conduction model to find the thermal conductivity. Because the thermal conductivity measurements were performed with the samples in high vacuum, convection losses were negligible. Radiation losses were accounted for numerically for all presented data using formulations presented in Ref. 24 and were less than 17% for all samples.

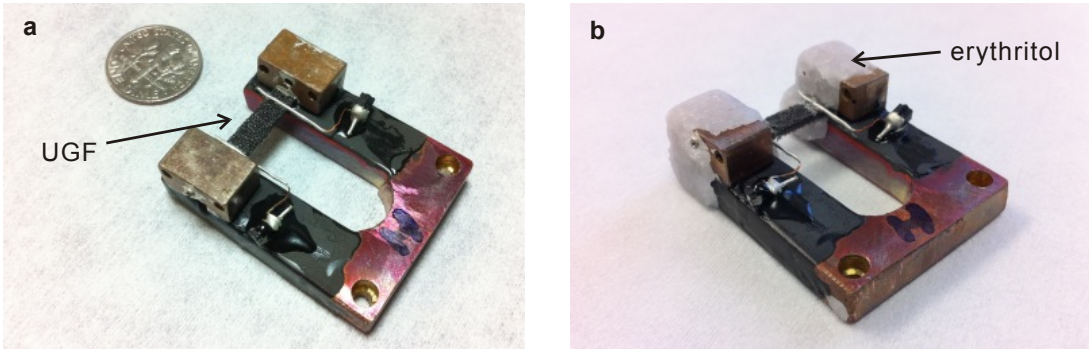

Figure S5. (a) Photograph of unfilled UGF sample mounted on a copper stage for thermal conductivity measurement. (b) Photograph of the same sample after erythritol loading.

Laser flash measurements. To measure the thermal conductivity of the pure PCMs, which are not electrically conductive, we first used a laser flash system (Netzsch LFA-457 micro flash) to measure the thermal diffusivity, $\alpha_{PCM}=\kappa_{PCM}\rho_{PCM}^{-1}C_{PCM}^{-1}$. We then calculated κ_{PCM} using the PCM specific heat, C_{PCM}, measured using differential scanning calorimetry (Netzsch DSC-404 F1 Pegasus), and the measured mass density, ρ_{PCM}.

Steady-state reference measurements. We measured the thermal conductivity of an erythritol-filled UGF composite sample using the steady state reference method to compare to our self-electrical-heating results. An un-annealed UGF-erythritol composite sample (φ_{foam}= 1.23±0.02%, ϕ_{PCM} = 84±0.4%) with 4 mm x 1.6 mm cross-section and 9.3 mm length (black bar) is connected to a constantan bar reference with 4 mm diameter and 12.5 mm length (grey bar) as show in Fig. S6. The assembly was sandwiched between a 50-ohm resistance heater (top of assembly) and a copper heat sink (bottom of assembly) to establish a linear temperature profile, which was measured using two 0.03 mm diameter differential Type-T thermocouples (blue and red wires). By assuming that the heat flux through the UGF-erythritol composite sample was the same as that through the constantan reference, we calculate the thermal conductivity of the sample using: $\kappa_{sample} A_{sample}\Delta T_{sample}/\Delta x_{sample}= \kappa_{constantan} A_{constantan}\Delta T_{constantan}/\Delta x_{constantan}$. The measurements were performed in high vacuum to minimize convective losses, and radiation losses were accounted for numerically using a fin model that can found on page 144 in Chapter 3 of *Introduction to Heat Transfer* by T.L. Bergman, A.S. Lavine, D.P. DeWitt, F.P. Incropera (John Wiley & Sons, NJ; 2006). When radiation loss is considered, the heat flux through a fin can be described by

$$q_{rad} = M\frac{(\cosh mL-\theta_L/\theta_b)}{\sinh mL}, \qquad (1)$$

where $\theta = T - T_\infty$, $\theta_b = T_b - T_\infty$, $M^2 = hP\kappa A_c\theta_b$, $m^2 = hP/\kappa A_c$, h is the effective radiation heat transfer coefficient defined as $h=4\varepsilon(T_0)\sigma T_\infty^3$, where *σ is the Stefan-Boltzmann constant* and $\varepsilon(T_\infty)$ is the sample emissivity (see Ref. 24 for details), P is the sample perimeter, A_c is the sample cross sectiona area. T_b is the tempearture at x = 0, T_L is the temperature at $x = L$, and T_∞ is the temperature of the surroundings. The UGF-PCM sample/constantan sandwich is then modeled using two fin equations by setting $T_L^{sample} = T_b^{constantan}$. The temperature of the heat sink, $T_L^{constantan}$, is set to be the stage temperature that was measured using a calibrated thermal diode during the experiment. The measured temperature gradients are used to obtain the temperature of the heater, T_b^{sample}. We take the limit of Eq. 1 as m→0 to find the case where radiation heat transfer becomes negligible. We compare the heat flux

through the sample/constantan sandwich when radition is considered to that when radiation is negligible to assess the error associated with neglecting radiation, which was found to be around 17% for the sample measured here. The heat lost through the heater leads (copper wires) and Type-T thermocouple wires were also accounted for numerically using the fin model and found to be around 5% of the total heat flux through the sample/constantan reference. The thermal conductivity of the UGF-erythritol composite is 2.8 ±0.3 W m^{-1} K^{-1} after correcting for all losses.

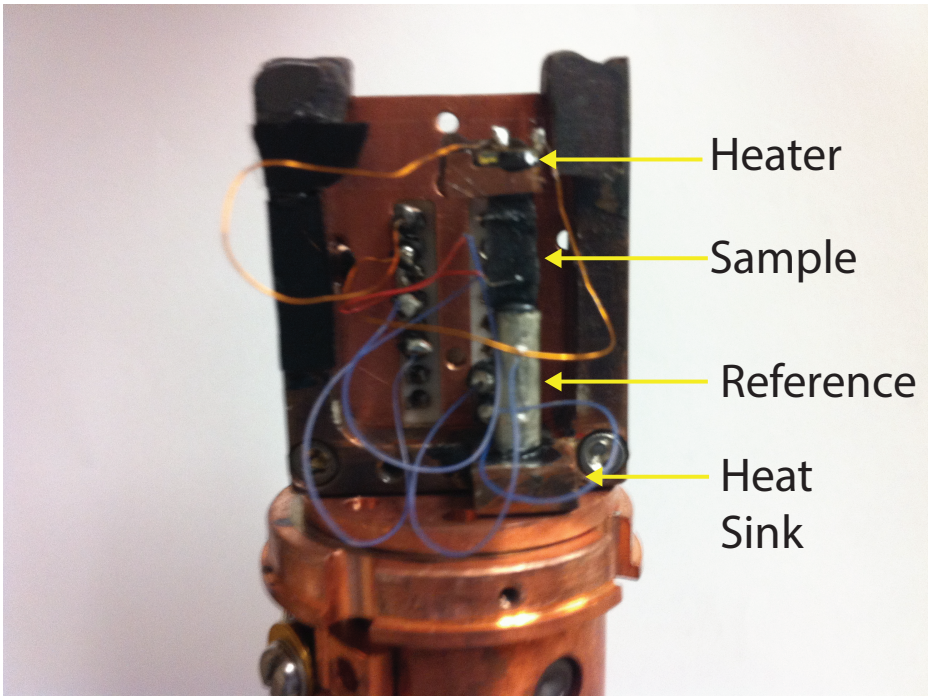

Figure S6. Photograph of steady state thermal conductivity measurement setup.

Table S1. Measured thermal properties of the unfilled UGFs, pure PCMs, and UGF-composites. The thermal conductivity values are results measured near the room temperature.

Unfilled Ultrathin-graphite Foam	Foam Solid Volume Fraction, ϕ_{foam}	κ_{foam} Measured [W m^{-1} K^{-1}]	κ_{strut} Calculated [W m^{-1} K^{-1}]
Annealed Foam1	1.23±0.03 vol.%	3.44±0.20	840
Un-annealed Foam1	0.83±0.02 vol.%	1.47±0.09	533
Un-annealed Foam2	0.88±0.02 vol.%	1.48±0.09	504

Pure Phase Change Material	Melting Temperature, T_m [deg. C]	Mass Specific Heat of Fusion, ΔH_{fus} [J g^{-1}]	κ_{PCM} Measured [W m^{-1} K^{-1}]
Paraffin Wax	58.9	189.3±5.7	0.20±0.02
Erythritol	120.2	338.5±10.2	0.81±0.09

Ultrathin-graphite Foam/ Phase Change Material Composite	PCM Filling Fraction, φ_{PCM}	Mass Specific Heat of Fusion, ΔH_{fus} [% of Pure PCM]	κ_{comp} Measured [W m^{-1} K^{-1}]	κ_{comp} Calculated [W m^{-1} K^{-1}]	κ_{comp} / κ_{PCM}
Annealed Foam1+ Wax	85.9±2.1 vol.% (96.4±2.4 wt.%)	98.2±3.5%	3.61±0.20	3.61	18.0
Un-annealed Foam1+ Wax	88.0±2.2 vol.% (97.6±2.4 wt.%)	100.8±3.5%	1.65±0.10	1.65	8.2
Un-annealed Foam2+ Erythritol	77.0±1.9 vol.% (98.2±2.5 wt.%)	98.5±3.5%	2.11±0.13	2.10	2.6

Infrared imaging analysis. We used a high-resolution science grade infrared (IR) camera (A655sc, Flir) to image the temperature gradient of UGF-wax composite and pure wax samples as they were heated from one side. The IR camera was calibrated for the UGF-wax composite and pure wax samples using a type-E thermocouple. The calibrated temperature curves are shown in Supplementary Fig. S7a and S7b. A copper plate with a length of 14 cm and thickness of 0.5 cm was attached to a hotplate (ECHOTHERM™ HS60) using a thermally conductive epoxy

and provided a large thermal mass. The copper plate was heated to a surface temperature of 105 °C as measured by a type-E thermocouple. Three Teflon holders with wall thickness of 250 μm were attached to copper foil with thickness of 0.2 mm using thermally conductive epoxy, and then loaded with: (i) pure wax sample, (ii) un-annealed UGF-wax sample, and (iii) annealed UGF-wax sample. The holders was made of 250 μm-thick Teflon (κ = 0.25 W m^{-1} K^{-1}). The thermal conductance of the holder is one tenth that of the 2 mm-thick pure wax sample. For the two composite samples, the foam was attached to the copper foil end plate using thermally conductive epoxy before loading with wax to ensure adequate thermal contact. The copper foil end plate was then attached to the hotplate (Supplementary Fig. S8), which was maintained at T = 105 °C. The IR images were acquired at a rate of 1 frame per second. Supplementary Video 2 shows the sample temperature change during the 600-second long measurement, which began at the moment immediately after the sample was attached to the heated copper plate.

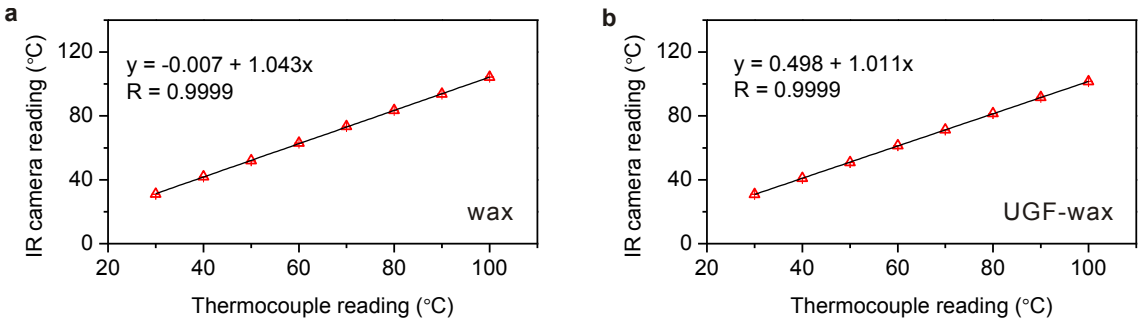

Figure S7. Temperature calibration curves for IR camera imaging of (a) pure wax and (b) UGF-wax composite performed using an E-type thermocouple. The obtained IR temperature measurement data reported in Fig. 5 has been multiplied by the corresponding slope of the calibration curve.

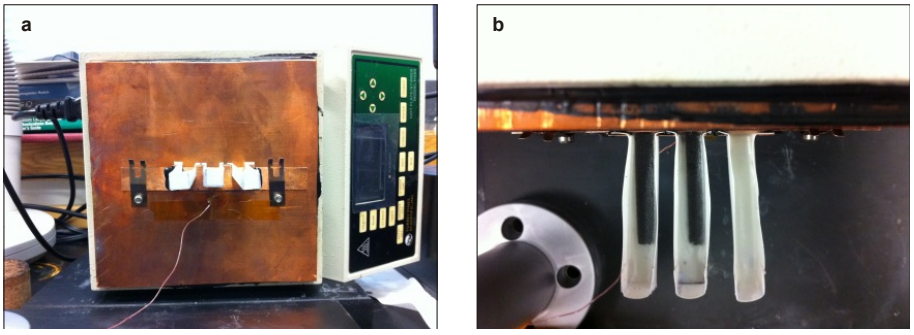

Figure S8. Photographs show (a) front view and (b) top view of the measurement setup for IR imaging. The copper plate was attached to a hot plate and used to provide a constant temperature source.

One-dimensional phase change model. The 1D phase change model used to generate the model data in Fig. 5e can be found on page 143 in *Heat Conduction* by L.M. Jiji (Begell House, New York; 2003). The model is based on Neumann's solution for melting of a semi-infinite region, where the solid-liquid interface location and temperature distribution is

$$x_i = \lambda\sqrt{4a_L t} \tag{2}$$

$$T_L(x,t) = T_b + \frac{(T_f - T_b)}{\operatorname{erf}\lambda}\operatorname{erf}\frac{x}{\sqrt{4a_L t}} \tag{3}$$

and

$$T_S(x,t) = T_\infty + \frac{(T_f - T_b)}{1-\operatorname{erf}\lambda}\left(1 - \operatorname{erf}\frac{x}{\sqrt{4a_S t}}\right), \tag{4}$$

where λ is the solid-liquid interface location away from the hot boundary, T_b.

$$\frac{\exp(-\lambda^2)}{\operatorname{erf}\lambda} - \sqrt{\frac{a_L}{a_S}}\frac{\kappa_S}{\kappa_L}\frac{T_f - T_\infty}{T_b - T_f}\frac{\exp\left(-\frac{a_L\lambda^2}{a_S}\right)}{1-\operatorname{erf}\left(\sqrt{\frac{a_L}{a_S}}\lambda\right)} = \frac{\sqrt{\pi}\Delta H_{fus}\lambda}{C_L(T_b - T_f)}. \tag{5}$$

Here, T_L and T_S are the temperature distribution in the liquid and solid, T_f is the temperature at the interface, T_∞ is the temperature far away from the hot surface (x = ∞), α_L and α_S are the thermal diffusivities of the liquid and solid, and C_L is the specific heat of the liquid. Like the IR measurement, in the model the entire sample is initially at room temperature T_∞, which is below the melting temperature, T_m. The surface at x = 0 is then suddenly maintained at a constant temperature, T_b, which is above the melting temperature. The liquid-solid interface forms instantaneously at the x = 0 and propagates throughout the solid sample. The boundary opposite x = 0 is maintained at the initial temperature, T_∞. The model neglects heat transfer in the Teflon container, as well as radiative and convective losses from the sample and assumes that the properties of each the solid and liquid phases are uniform and remain constant. As input to the model, we used the measured heat of fusion, exact measurement geometry, and initial and boundary temperatures measured using an E-type thermocouple. Thermal diffusivities of the solid and liquid states for the UGF-wax composite samples were calculated using rule of mixtures and the measured diffusivity for the wax. The foam thermal conductivity required for rule of mixture calculation was obtained as $\kappa_{foam} = (\varphi_{foam}/3)\kappa_{strut}$ using the measured foam volume fraction of each UGF sample and the average solid strut thermal conductivity measured using the self-electrical heating method, κ_{strut} = 520 W m^{-1} K^{-1}.

Large scale UGF synthesis.

Figure S9 shows the large size ultrathin-graphite foam sample grown on a 4 inch inch-diameter quartz tube furnace. The growth parameters can be found above in the section: **Ultrathin-graphite foam (UGF) and composite synthesis.**

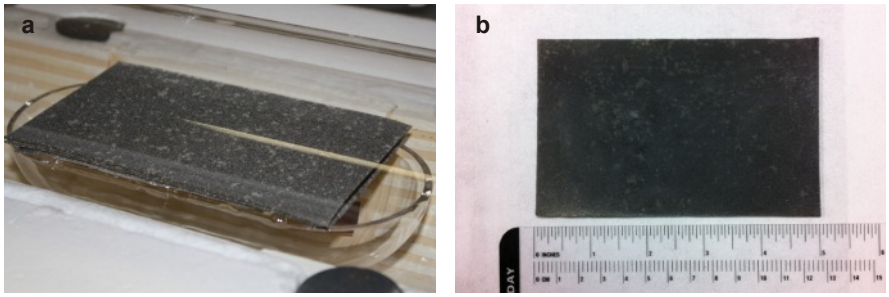

Figure S9. Photograph of (a) ultrathin-graphite grown on nickel foam located in growth furnace, and (b) UGF after removing nickel and loading with wax.